View metadata, citation and similar papers at core.ac.uk
brought to you by CORE
provided by UTHM Institutional Repository

Magnetic Flux Analysis of E-Core Hybrid Excitation Flux Switching Motor with Various Topologies

Siti Nur Umira Zakaria, Erwan Sulaiman
Center for Electromagnetic Compatibility
Universiti Tun Hussein Onn Malaysia
Locked Bag 101, 86400 Batu Pahat, Johor Malaysia
umirazakaria@yahoo.com, erwan@uthm.edu.my

Abstract—In this paper, magnetic flux analysis of E-Core hybrid excitation flux switching motor (HEFSM) with various slot-pole combinations are presented. With several advantages of concentrated armature and DC field excitation coil (DC-FEC) windings, variable flux capability and robust rotor structure, design feasibility and performances analysis of 6Slot-4Pole, 6Slot-5Pole, 6Slot-7Pole and 6Slot-8Pole E-Core HEFSMs such as flux lines, flux linkage, cogging torque and flux distribution are analyzed based on 2D Finite Element Analysis (2D-FEA). Further design improvements and optimizations will be performed in future to increase their performances in term of torque and power.

Keywords—hybrid excitation flux switching machine (HEFSM); permanent magnet (PM); concentrated winding; magnetic flux

I. E-Core HEFSMs Topologies

The development of E-Core HEFSM starts with evolution of conventional 12S-10P permanent magnet flux switching machine (PMFSM) as shown in Fig. 1. In Fig. 1(a) the salient pole stator core consists of modular "U-shaped" laminated segments which are placed circumferentially between alternate polarities of magnetized PMs. The stator winding comprises concentrated armature coils wounded on a stator pole formed by two adjacent laminated segments and a magnet. As compared with conventional PM brushless machines [1], the slot area is reduced when the magnets are moved from the rotor to the stator, but when liquid cooling is employed, temperature rise of the magnets may be more easily managed since it is very difficult to dissipate the heat from rotor of conventional machine. PMFSM may have all poles wound or alternate poles wound as depicted in Fig. 1(a) and (b), respectively. It is obvious that in an alternate pole wound, the torque reduces considerably when PM in stator poles without coils are eliminated. In order to reduce the PM usage and, consequently, the cost, the stator poles without coils are replaced by corresponding stator teeth. However since the PM in the stator poles which carry coils are magnetized in the same direction, their magnetic field is "short circuited" via the stator back-yoke. Consequently, the circumferentially magnetized magnets of alternate polarity are employed as illustrates in Fig. 1(c), which is designated as E-core PMFSM due to laminated "E-shape" segments employed in the stator. In contrast with conventional all pole wound PMFSM, the E-core PMFSM has the same rotor structure, less number of stator poles and half volume of PM.

Exploratory Research Grant Scheme, Vot No E030, Ministry of Higher Education, Malaysia

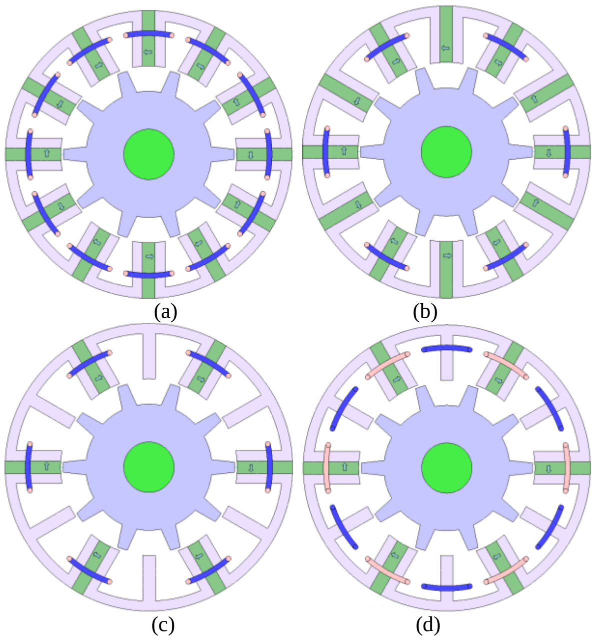

Fig. 1: Conventional and E-Core PMFSM (a) Conventional PMFSM with all pole wound. (b) Conventional PMFSM with alternative pole wound (c) E-Core PMFSM with alternate PM direction (d) E-Core HEFSM

The magnet and its two adjacent stator teeth are defined as one stator pole [1-2].

A new structure of 6S-10P E-Core HEFSM is designed by employing additional DC-FEC on the middle stator teeth of the E-Core PMFSM with no magnet as shown in Fig. 1(d) [3]. It sustains equivalent outer diameter as the corresponding E-Core PMFSM and exhibits a simpler 2D structure when compared with hybrid-excited PM machine developed from the conventional PMFSM. Since it also employs non overlap between DC-FEC and armature windings, the number of turns per phase of the E-Core HEFSM is maintained similar as that of the E-Core PMFSM. Moreover, the slot area in this machine is divided into two partitions, each for armature coil and DC-FEC windings, respectively. The total number of armature winding turns is equal to that of DC-FEC winding turns to ease the comparison of armature and field currents, because the slot areas for these two kinds of windings are equivalent. It is worth mentioning that, different with HEFSM developed from

978-1-4799-6603-5/14/$31.00 ©2014 IEEE

conventional PMFSM [4], the PM DC-FEC in the designed E-Core HEFSM remains similar as that in the conventional E-Core PMFSM. With additional DC-FEC employs in the designed motor, variable flux control capability can easily be applied to the E-Core HEFSM for various performances when compared with constant flux of PM in PMFSM.

II. Operating Principle of E-Core HEFSM

The operating principle of E-Core HEFSM is similar with conventional flux switching machine (FSM) in which the flux flows from the stator to the rotor switches its polarity following the rotation of rotor. At one instant, half of rotor poles receive the flux from the stator while another half of rotor poles bring the flux to the stator to make a complete flux cycle. The operating principle and definition of flux switching can be described either by changing flux in the stator or changing flux in the rotor. Fig. 2 illustrates the operating principle of E-Core HEFSM in three different conditions. In Fig. 2(a), both fluxes of PM and DC-FEC flow from stator to rotor pole P2 and return back to the stator by rotor pole P1. At this stage, it is obvious that rotor pole P2 received the flux from stator. Meanwhile, in Fig. 2(b), when the rotor moves to the left side approximately half electric cycles, both fluxes from stator flow to rotor pole P3 in between DC-FEC winding of right side. It is clear that the stator flux switches its polarity through rotor pole P3 as receiving flux while rotor pole P2 brings the flux back to the stator to form a complete flux cycle. Finally, Fig. 2(c) depicts the condition where rotor pole P3 is in similar condition with rotor pole P2 in Fig. 2(a) to form one electric cycle. At this stage, the flux from stator flows through stator teeth between PM and armature coil to rotor pole P3 while rotor pole P2 brings the flux to the stator, simultaneously. Since the direction of both PM and FEC fluxes are in the same polarity, both fluxes are combined and move together into the rotor, hence producing more fluxes with a so called hybrid excitation flux [5-6].

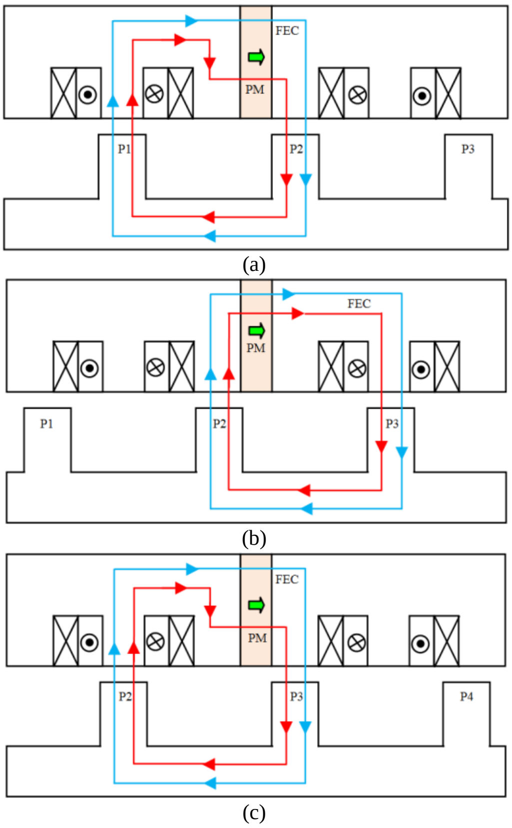

Fig. 2: Principle operation of E-Core HEFSM (a) flux from stator via P2 and P1 (b) flux from stator via P3 and P2 (c) flux from stator via P3 and P2 for one electric cycle

III. Design Restriction and Specification

In this paper, design study and flux interaction analysis between DC-FEC and armature coil of 6Slot-4Pole, 6Slot-5Pole, 6Slot-7Pole and 6Slot-8Pole E-Core HEFSM are investigated. The main geometrical dimensions of the designed E-Core HEFSM are identical with IPMSM used in conventional electric vehicle in which the stator outer diameter and stack length are set to 132mm and 70mm, respectively. Fig. 3 shows the motor with initial dimension of main machine parts including air gap, stator outer and inner diameter, rotor outer and inner diameter and shaft diameter.

The design requirements, restrictions and target specifications of the E-Core HEFSMs are listed in Table 1, similar with the available and estimated specifications with IPMSM [7]. The electrical restrictions related with the inverter such as maximum 650V DC bus voltage and maximum 360V inverter current are set to be much severe. Assuming that only a water-jacket system is employed as the cooling system of the machine, the limit of the current density is set to 30A_{rms}/$mm^2$and 30A/$mm^2$for both armatur**e** winding and DC-FEC respectively. Additionally, the PM weight is limited to maximum of 1.0Kg where Neomax35AH having coercive force at 20°C and residual flux density of 932kA/m and 1.2T, respectively is used as PM material while the electrical steel 35H210 is used for the stator and rotor body. The rotor structure is mechanically robust to rotate at high speed because it consists of only stacked electromagnetic sheets and hence, it is highly possible to elevate the target maximum operating speed up to 12,400r/min while keeping enough rotor mechanical strength. The target maximum torque and power are 333Nm and 123KW respectively, determined from a realization of comparable with the present IPMSM.

IV. Performances Prediction of Initial E-Core HEFSM Based on Two-Dimensional FEA

The performance predictions of the designed E-Core

TABLE 1. E-Core HEFSM Design Specifications

Items	E-Core HESFM
Maximum DC voltage (V)	650
Maximum current (A_{rms})	360
Maximum J_a (A_{rms}/mm^2)	30
Maximum J_e (A/mm^2)	30
Stator diameter (mm)	264
Machine length (mm)	70
Diameter of shaft (mm)	60
Air-gap (mm)	0.8
PM volume (kg)	1.0
Max. speed (r/min)	12,000
Max. torque (Nm)	333
Max. power (kW)	123
Power density (kW/kg)	3.5

HEFSMs are conducted using commercial 2D-FEA package, JMAG-Studio ver.13.0, released by Japanese Research Institute. Primarily, the rotor, stator, armature coil, DC-FEC and PM of the proposed 6Slot-4Pole, 6Slot-5Pole, 6Slot-7Pole and 6Slot-8Pole E-Core HEFSMs are sketched in Geometry-Editor. Then, the area of armature coil, S_a and the area of DC-FEC, S_e are used to calculate optimum natural number of turns of armature coil, N_a and DC-FEC, N_e, respectively. Besides, the materials, conditions, circuits and properties of the machine are set in JMAG-Designer. Moreover, performance characteristics in open circuit such as coil arrangement test, hybrid excited flux characteristics, cogging torque, flux linkage and flux distribution are analyzed in this design.

A. Flux Linkage of PM and Cogging Torque

Under open circuit condition, the flux paths of PM for 6Slot-4Pole, 6Slot-5Pole, 6Slot-7Pole and 6Slot-8Pole E-Core HEFSMs at zero degree rotor position are compared as illustrated in Fig. 3. From the figure, all fluxes flow from stator to rotor and return through adjacent rotor teeth to make a complete six flux cycles. In addition, most of the generated fluxes are distributed uniformly around the stator and rotor poles with average flux density of 2.8T. However, the fluxes generated are slightly saturated at rotor air gap and stator outer yoke with maximum magnetic flux density of approximately 3T. Thus, from design point of view, the rotor air gap can be reduced to decrease the flux leakage, while the stator outer yoke width can be increased to reduce the flux saturation.

The generated PM flux linkages are also compared as depicted in Fig. 4 for all designs. It is noticeable that 6S-4P design has the highest magnetic flux amplitude of 0.056Wb, while 6Slot-5Pole and 6Slot-7Pole designs have similar flux characteristics with flux amplitude of approximately 0.049Wb, and 6Slot-8Pole design has the lowest magnetic flux with

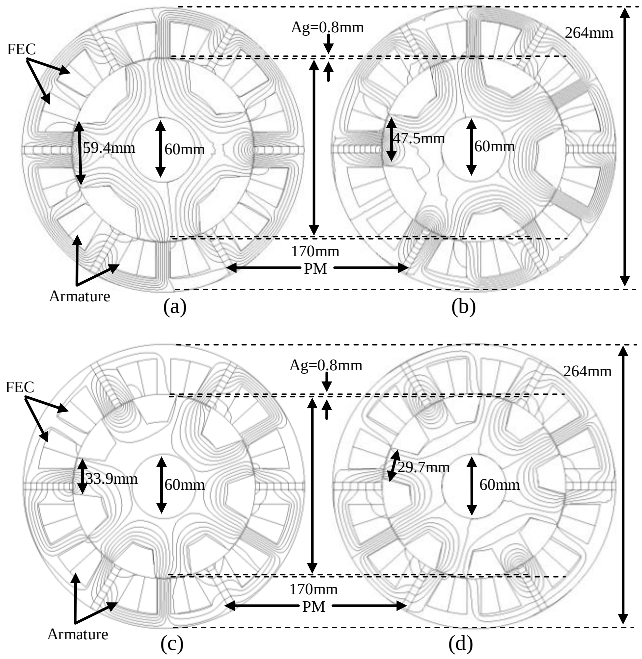

Fig. 3. Main machine dimension and flux line of various slot-pole combinations (a) 6Slot-4Pole (b) 6Slot-5Pole (c) 6Slot-7Pole (d) 6Slot-8Pole

approximately half of 6Slot-4Pole design. It is observed that increasing the rotor pole number results in low flux generation due to separation of flux in all rotor teeth. In addition, the flux characteristics of 6Slot-4Pole and 6Slot-8Pole designs are much distorted when compared with 6Slot-5Pole and 6Slot-7Pole designs due to fairly significant difference between slot-pole combinations. Fig. 5 illustrates the comparisons of no-load cogging torque of all designs E-Core HEFSM. From the plot, less amount of cogging torque with approximately 4Nm peak-to-peak for 6Slot-7Pole is produced due to slightly sinusoidal magnetic flux linkage compared to other number of rotors. Since the peak-peak torque generated should generally not exceed more than 10% of the average torque to avoid high vibration and noise, further design refinement should be conducted to get the best performance of the machine. It is noticeable that most of the flux linkage waveforms are distorted with large amount of cogging torque pulsation due to

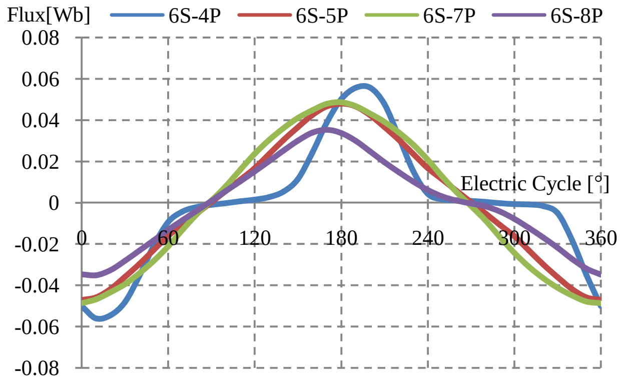

Fig. 4. PM Flux linkage of E-Core HEFSMs

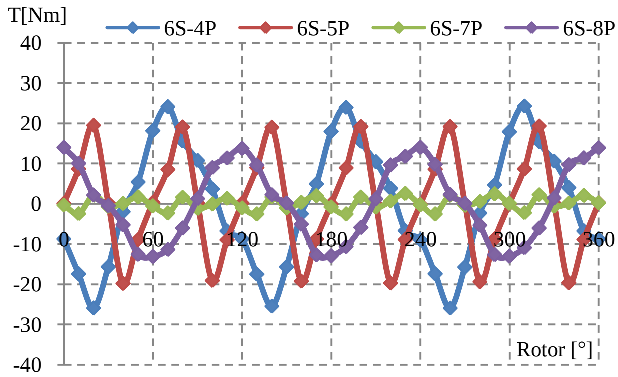

Fig. 5. Cogging torque of the initial design

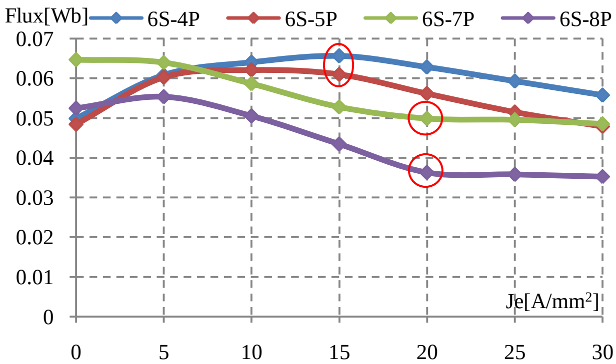

Fig. 6. PM and DC-FEC flux linkage at various J_e

the fifth harmonic order that occurs in the initial flux itself.

B. Flux Linkages of PM with DC-FEC at Various J_e

The flux linkage combinations of both PM and DC-FEC at various DC-FEC current densities are also investigated as shown in Fig. 6. From the plot, 6Slot-4Pole and 6Slot-5Pole designs give similar flux characteristics in which the fluxes keep increasing until J_e of 15A/mm^2 and start to reduce when higher J_e is inject to the system. In addition, at J_e of 0A/mm^2, although the flux generated from 6Slot-7Pole and 6Slot-8Pole designs are higher than 6Slot-4Pole and 6Slot-5Pole designs, it is evident that flux from DC-FEC cancelled all the PM flux and become saturated at J_e of 20A/mm^2 as clearly shown in red circle. To explain this phenomenon, further investigations of short circuit field distribution based on 2D-FEA for PM with Je at three conditions such as (a) before the maximum flux, (b) at maximum flux, and (c) after the maximum flux are analyzed. For example for 6Slot-4Pole, details investigation into flux distribution at J_e of 5A/mm^2, 15A/mm^2 and 30A/mm^2 is made as shown in Fig. 7. From the flux vector diagram, it can be seen that for low Je of 5A/mm^2 the flux can easily flow to the direction according to its principle as shown in Fig. 7(a). In this condition, some of J_e flux has been cancelled by PM flux as shown in red circle. It is notice that the dominant PM flux flows in the stator tooth between FEC coil slots to the rotor hence making one complete cycle flux. Nevertheless, when J_e is increased to 15A/mm^2, higher J_e flux cancels PM flux at stator tooth between DC-FEC as shown in Fig. 7(b). However at much higher J_e of 30A/mm^2, flux from DC-FEC becomes dominant in this system and cancelled flux from PM thus produces lowest magnetic flux compared to J_e of 5A/mm^2 as represent in Fig. 7(c).

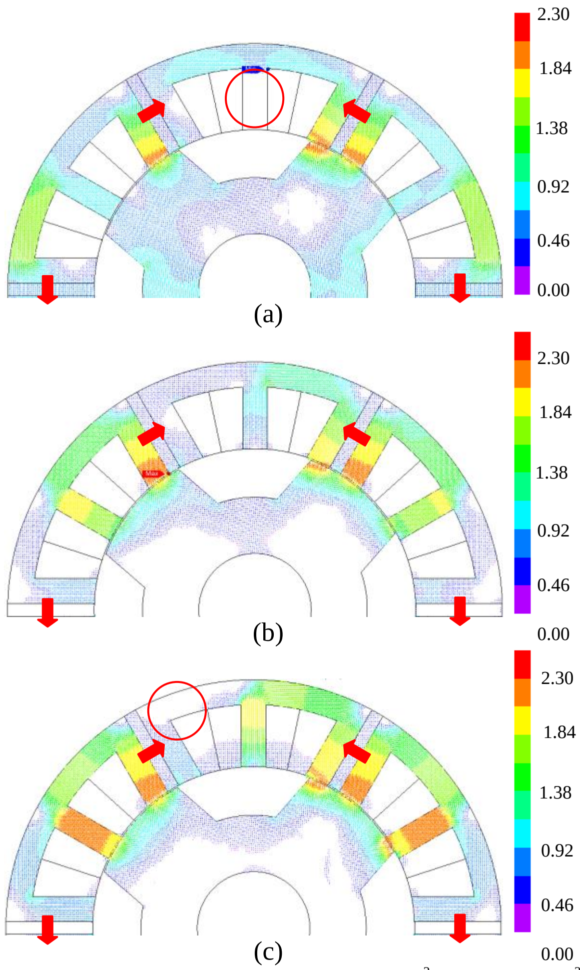

Fig. 7: Flux vector diagram at various J_e (a) J_e=5A/mm^2 (b) J_e=15 A/mm^2 (c) J_e=30A/mm^2

V. CONCLUSION

Design possibility studies and performance investigation of 6Slot-4Pole, 6Slot-5Pole, 6Slot-7Pole and 6Slot-8Pole E-Core HEFSMs topologies are presented in this paper. The operating principle of DC-FEC, PM and armature windings placed on the stator has been analyzed. The performances of the E-Core HEFSM such as magnetic flux capability have been examined. To prove the operating principle and to validate each coil phase, the coil arrangement test for this design has been examined. The machine has the advantages of easy manufacturing, low copper loss and cost due to less volume of PM and less DC-FEC respectively. Finally, the proposed E-Core HEFSM is suitable for various applications with various performances.

REFERENCES

[1] J. T. Chen, Z. Q. Zhu, S. Iwasaki, and Rajesh P. Deodhar, “A Novel E-Core Switched-Flux PM Brushless AC Machine;” IEEE Transactions on Industry Application, vol. 47, no. 3, May/June 2011

[2] J. T. Chen, Z. Q. Zhu, S. Iwasaki, and R. Deodhar: “Comparison of losses and efficiency in alternate flux-switching permanent magnet machines”, XIX Int. Conf. on Elec. Machines, ICEM 2010, Sept. 2010

[3] C. C. Chan, and K. T. Chau: “An overview of power electronics in electric vehicles,” IEEE Trans. Ind. Electron., vol. 44, no. 1, pp.3–13, Feb. 1997

[4] J. T. Chen, Z. Q. Zhu, S. Iwasaki, and Rajesh P. Deodhar, “Novel Hybrid-Excited Switched-Flux Brushless AC Machine for EV/HEV Applications, ”IEEE Transactions on Vehicular Technology, vol.60, no. 4, May 2011

[5] E. Sulaiman, T. Kosaka, N. Matsui, and M. Z. Ahmad, “Design Studies on High Torque and High Power Density Hybrid Excitation Flux Switching Synchronous Motor for HEV Applications,” IEEE International Power Engineering and Optimization Conferences (PEOCO2012), June 2012

[6] M. Z. Ahmad, Z. A. Haron and E. Sulaiman, “Design Studies on 12S-10P Outer-Rotor HEFSM for In-Wheel Drive EV Applications,” IEEE Conference on Sustainable Utilization and Development in Engineering and Technology, May 2013

[7] M. Kamiya, “Development of Traction Drive Motors for the Toyota Hybrid Systems,” *IEEJ Transactions on Industry Applications*, Vol. 126, No. 4, Sec. D, 2006, pp. 473-479.